Tetrahedron 70 (2014) 7429–7438

Contents lists available at ScienceDirect

Tetrahedron

journal homepage: www.elsevier.com/locate/tet

Solvent-dependent chromogenic sensing for Cu^{2+} and fluorogenic sensing for Zn^{2+} and Al^{3+}: a multifunctional chemosensor with dual-mode

Gyeong Jin Park [a], Dae Yul Park [a], Kyung-Min Park [b], Youngmee Kim [c], Sung-Jin Kim [c], Pahn-Shick Chang [b,*], Cheal Kim [a,*]

[a] Department of Fine Chemistry and Department of Interdisciplinary Bio IT Materials, Seoul National University of Science and Technology, Seoul 139-743, Republic of Korea
[b] Department of Agricultural Biotechnology, Center for Food and Bioconvergence, and Research Institute of Agriculture and Life Sciences, Seoul National University, Seoul 151-742, Republic of Korea
[c] Department of Chemistry and Nano Science, Ewha Womans University, Seoul 120-750, Republic of Korea

ARTICLE INFO

Article history:
Received 26 June 2014
Received in revised form 11 August 2014
Accepted 12 August 2014
Available online 17 August 2014

Keywords:
Copper ion
Zinc ion
Aluminum ion
Colorimetric
Fluorescent
Reversible

ABSTRACT

A new multifunctional chemosensor **1** was synthesized and characterized by spectroscopic tools along with a single crystal X-ray crystallography. It can exhibit selective recognition responses toward Cu^{2+}, Zn^{2+} and Al^{3+} in different solvent systems with bimodal methods (colorimetric and fluorescence). This sensor **1** detected Cu^{2+} ions through a distinct color change from colorless to yellow in aqueous solution. Interestingly, the receptor **1** was found to be reversible by EDTA. The detection limit (11 μM) of **1** for Cu^{2+} is much lower than WHO guideline (30 μM) in drinking water. In addition, the sensor **1** showed significant fluorescence enhancements in the presence of Zn^{2+} ion and Al^{3+} ion in two different organic solvents (DMF and MeCN), respectively. The binding modes of the three complexes were determined to be a 1:1 complexation stoichiometry through Job plot, ESI-mass spectrometry analysis, and ^1H NMR titration.

© 2014 Elsevier Ltd. All rights reserved.

1. Introduction

Unlike other traditional methods (e.g., inductively coupled plasma atomic emission spectrometry,[1] atomic absorption spectroscopy,[2] and electrochemical methods[3]), chemosensors are highly estimable means for the selective recognition of chemical and biological species in environmental chemistry and biology.[4] The design and construction of colorimetric and fluorescent chemosensors with high selectivity and sensitivity for trace metal ions, such as copper, zinc, and aluminum, are currently of great importance as they allow nondestructive and prompt detection of metal ions by a simple absorbance and fluorescence enhancement (turn-on) response.[5] Among the various types of chemosensors, the chromogenic chemosensors are also widely used owing to the inexpensive equipment required or no equipment at all.[6] Furthermore, fluorescence sensors are excellent tools for detecting metal ions due to their high sensitivity, good selectivity, high response speed and simple operation.[6a,b]

Copper, as the third most abundant essential trace element in the human body, performs an important role in many fundamental physiological processes in organisms.[7] However, with excessive loading, copper ion can cause extremely negative health effects such as gastrointestinal disturbance and liver or kidney damage.[8] Zinc, the second most abundant transition metal, is fundamental in biology systems.[9] In a human body, it is well known that many catalytic centers and structural cofactors are composed of several Zn^{2+}-containing enzymes and DNA-binding proteins.[10] Excess zinc, however, can cause various intoxications and a number of severe neurological diseases (e.g., Alzheimer's disease, cerebral ischemia, and epilepsy), developmental defects, and malfunctions.[11] Aluminum has been identified as a neurotoxin over one hundred years, and can cause health hazards like Alzheimer's disease and osteomalcia, and even contribute to the risk of cancer of the breast.[12] Therefore, the development of new analytical methods for the selective determination of Cu^{2+}, Zn^{2+}, and Al^{3+} is highly desirable. Up to now, a number of colorimetric and fluorescent chemosensors for Cu^{2+}, Zn^{2+} or Al^{3+} have been reported.[13] However, most of the

* Corresponding authors. Tel.: +82 2 970 6693; fax: +82 2 973 9149 (C.K.); tel.: +82 2 873 5095; fax: +82 2 880 4852 (P.S.C.); e-mail addresses: pschang@snu.ac.kr (P.-S. Chang), chealkim@seoultech.ac.kr, chealkim20@daum.net (C. Kim).

http://dx.doi.org/10.1016/j.tet.2014.08.026
0040-4020/© 2014 Elsevier Ltd. All rights reserved.

reported fluorescent chemosensors can selectively sense only one of them. Therefore, single chemosensors for multiple analytes have recently become very popular among the analysts, because of their fast detection time and cost reduction.[14] For example, they include Cr^{3+}/Al^{3+},[15a] Cu^{2+}/Hg^{2+},[15b] Zn^{2+}/Cd^{2+},[15c] and Al^{3+}/Fe^{3+}.[14a]

The julolidine group is a well-known chromophore and chemosensors with the julolidine moiety are usually water-soluble.[16] In addition, the antipyrine moiety is one of the biologically important moieties with good optical properties.[17] We expected that the combination of the julolidine and the antipyrine groups might show good chromogenic or fluorogenic responses to metal ions. Moreover, the combination form of the julolidine and the antipyrine moieties has three potential binding sites (a nitrogen atom of imine and two oxygen atoms of julolidine and antipyrine), which might act as a strong coordination donor toward metal ions. Therefore, we combined these two moieties to make a new chemosensor, and tested its sensing properties. Importantly, receptor **1** exhibited selective recognition responses toward Cu^{2+}, Zn^{2+} and Al^{3+} in different solvent systems with bimodal methods (colorimetric and fluorescence).

Herein, we report a new Schiff base with both a julolidine group and an antipyridine one, which acts as a colorimetric and fluorescent chemosensor for detection of Cu^{2+}, Zn^{2+} and Al^{3+} in a dual-channel mode (naked-eye and fluorescence emission). In the presence of Cu^{2+}, the chemosensor **1** showed an instant color change from colorless to yellow in the DMSO-buffer solution. Moreover, this sensor **1** displayed fluorescence enhancements in the presence of Zn^{2+} and Al^{3+} in DMF and MeCN, respectively.

2. Results

2.1. Synthesis, characterization and solvent-dependent sensing properties of 1

A new chemosensor **1** was obtained by the condensation reaction of 8-hydroxyjulolidine-9-carboxaldehyde with 4-aminoantipyrine in ethanol at room temperature (Scheme 1), and characterized by ^{1}H NMR, ESI-mass spectrometry analysis, elemental analysis, and X-ray crystallography.

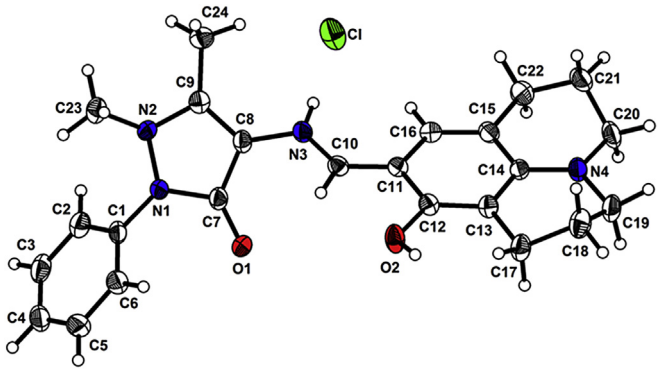

Fig. 1. Crystal structure of **1**·HCl. Displacement ellipsoids are shown at the 50% probability level.

Co^{2+}, Ni^{2+}, Cu^{2+}, Zn^{2+}, Al^{3+}, Ag^{+}, Cd^{2+}, Hg^{2+}, and Pb^{2+} with their nitrate salts in DMSO-buffer solution (2:1, v/v, 10 mM bis–tris, pH 7.0) at room temperature. As shown in Fig. 2, only Cu^{2+} ion induced a distinct spectral change (Fig. 2a) and an instant color change (Fig. 2b) from colorless to yellow, while other metal ions did produce little or no changes. This result indicated that receptor **1** can serve as a potential candidate of a 'naked-eye' chemosensor for Cu^{2+} in aqueous solution.

To further investigate the chemosensing properties of **1**, UV–vis titration of **1** with Cu^{2+} was performed (Fig. 3). Upon the addition of Cu^{2+} to a solution of **1**, the absorbance at 405 nm gradually decreased and a new absorbance at 442 nm appeared concomitantly. The red shift ($\Delta\lambda_{abs}$=37 nm) of the absorption band could be explained by internal charge transfer (ICT) mechanism. Kaur et al. suggested that ICT mechanism referred to the push–pull effect of the electron donating ('push') and electron-withdrawing ('pull') groups.[18] Likewise, we assume that the red shift of **1**-Cu^{2+} complex was induced by binding of Cu^{2+} ion to the C=N group in the receptor **1** with the electron-donating group (tertiary amine in the julolidine group) and the electron-withdrawing one (imine moiety). Therefore, the change of ICT band might be responsible for the dramatic color change from colorless to yellow. The distinct isosbestic point was clearly observed at 416 nm, indicating the formation of the only one species between **1** and Cu^{2+}.

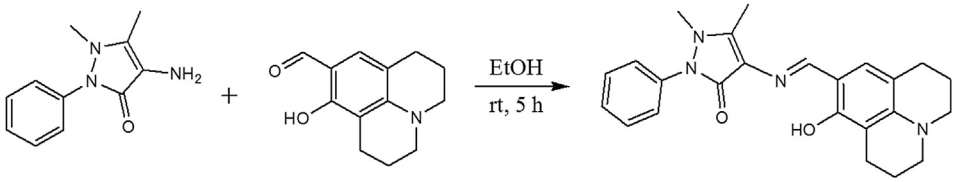

Scheme 1. The synthetic procedure for receptor **1**.

Crystals of **1** were obtained by slow evaporation in methanol and its structure is shown in Fig. 1. We tested sensing abilities of **1** towards various metal ions in several solvent systems such as MeOH, EtOH, DMSO, DMF, MeCN and their aqueous solutions. Noticeable change in the absorbance of **1** was observed in the presence of Cu^{2+} only in DMSO-buffer solution (2:1). In addition, the sensor **1** showed significant fluorescence enhancements in the presence of Zn^{2+} ion and Al^{3+} ion in two different organic solvents (DMF and MeCN), respectively. It is worthwhile to mention that **1** can sense Cu^{2+}, Zn^{2+}, and Al^{3+} ions, while most of the chemosensors reported for the three metal ions could selectively sense only one or two of them.

2.2. Chromogenic sensing for Cu^{2+} in aqueous solution

The chromogenic sensing ability of **1** was examined with various metal ions such as Na^{+}, K^{+}, Mg^{2+}, Ca^{2+}, Cr^{3+}, Mn^{2+}, Fe^{2+}, Fe^{3+},

Job plot analysis exhibited a 1:1 complexation stoichiometry for **1**-Cu^{2+} complex formation (Fig. S1), which was further confirmed by ESI-mass spectrometry analysis (Fig. 4).

The positive-ion mass spectrum of **1** upon addition of 1 equiv of Cu^{2+} showed the formation of **1**-Cu^{2+} complex [*m*/*z*: 541.80; calcd, 542.14]. Based on Job plot, ESI-mass spectrometry analysis and the crystal structures of similar type of Cu complexes reported in the literature,[19] we propose the structure of **1**-Cu^{2+} complex (Scheme 2).

The association constant for the **1**-Cu^{2+} complexation was determined as 5.0×10^4 M^{-1} through Benesi–Hildebrand equation (Fig. S2), which is in the range of those (1.0×10^3–1.0×10^{12}) previously reported for Cu^{2+}-binding chemosensors.[20] Based on the result of UV–vis titration, the detection limit ($3\sigma/k$) of the receptor **1** for the analysis of Cu^{2+} ion was calculated to be 11 μM (Fig. S3),

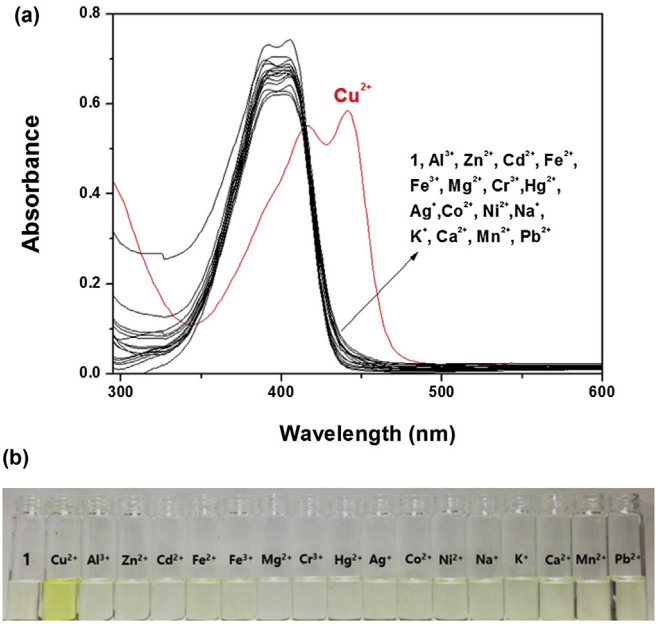

Fig. 2. (a) Absorption spectra change of **1** (20 μM) in the presence of various metal ions in DMSO-buffer solution (10 mM bis–tris, pH 7.0, 2:1, v/v). (b) Color change of receptor **1** (20 μM) in the presence of 4 equiv of metal ion in DMSO-buffer solution (10 mM bis–tris, pH 7.0, 2:1, v/v).

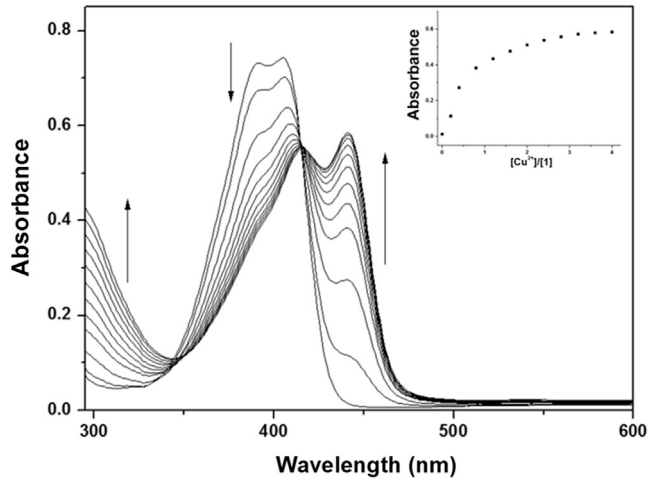

Fig. 3. UV–vis spectra of receptor **1** (20 μM) upon the addition of Cu^{2+} in DMSO-buffer solution (10 mM bis–tris, pH 7.0, 2:1, v/v). Inset: The ratio of absorbance of **1** as a function of Cu^{2+} equiv.

which is sufficient below the WHO guideline (30 μM) of Cu^{2+} in drinking water.[21] This result suggests that receptor **1** could be used as a powerful tool for detecting Cu^{2+} ion without expensive instruments.

To examine the interference of other relevant metal ions on **1**-Cu^{2+} complexation, the competition experiments were performed in the presence of Cu^{2+} mixed with other metal ions such as Na^{+}, K^{+}, Mg^{2+}, Ca^{2+}, Al^{3+}, Cr^{3+}, Mn^{2+}, Fe^{2+}, Fe^{3+}, Co^{2+}, Ni^{2+}, Zn^{2+}, Ag^{+}, Cd^{2+}, Hg^{2+}, and Pb^{2+} (Fig. 5). Upon the addition of 4 equiv of Cu^{2+} ion in the presence of the same concentration of other metal ions, the coexistent metal ions did not interfere with naked-eye detection of Cu^{2+} by the receptor **1** in aqueous media. Thus, receptor **1** could be used as a selective colorimetric sensor for Cu^{2+} in the presence of most competing metal ions.

The effect of pH on the absorption response of receptor **1** to Cu^{2+} ions was investigated in the pH range of 2–12 (Fig. S4). The color of

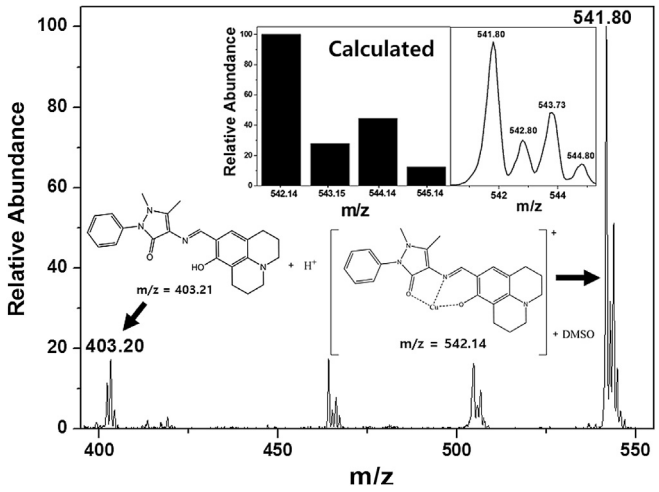

Fig. 4. Positive-ion electrospray ionization mass spectrum of **1** (0.1 mM) upon addition of Cu^{2+} (0.1 mM) in a mixture of MeCN/DMSO (9:1).

the **1**-Cu^{2+} complex exhibited the intense and stable absorption intensities between pH 4 and pH 11, which warrant that Cu^{2+} could be clearly detected by the naked eye or UV–vis absorption measurements using receptor **1** over a wide pH range of 4–11.

To examine the reversibility of receptor **1** toward Cu^{2+}, ethylenediaminetetraacetic acid (EDTA) (4 equiv) was added to the complexed solution of receptor **1** and Cu^{2+}. As shown in Fig. 6, the addition of EDTA to a mixture of **1** and Cu^{2+} resulted in return of the absorbance with colorless at 450 nm, which indicates the regeneration of the free **1**. Upon addition of Cu^{2+} into the solution again, the color and the absorbance were recovered. The color change (Fig. 6a) and absorbance (Fig. 6b) were almost reversible even after several cycles with the sequentially alternative addition of Cu^{2+} and EDTA. These results indicate that the receptor **1** could be used as a reversible colorimetric chemosenor in aqueous solution.

2.3. Fluorogenic sensing for Zn^{2+} in DMF

We have also examined the selectivity of **1** toward a variety of metal ions through fluorescence emission in DMF at room temperature. As shown in Fig. 7, the receptor **1** alone has a very weak fluorescence emission with an excitation of 430 nm. When 8 equiv of various metal ions such as Na^{+}, K^{+}, Mg^{2+}, Ca^{2+}, Al^{3+}, Cr^{3+}, Mn^{2+}, Fe^{2+}, Fe^{3+}, Co^{2+}, Ni^{2+}, Zn^{2+}, Ag^{+}, Cd^{2+}, Hg^{2+}, and Pb^{2+} with their nitrate salts was added to the receptor **1**, it was found that the solution of **1** exhibited no or small significant increase of the fluorescence except Zn^{2+} and Al^{3+}. The addition of Zn^{2+} resulted in drastic enhancements of the emission intensities at 500 nm (200-folds). Meanwhile, the addition of Al^{3+} into **1** also showed the increase in the fluorescence intensity at 485 nm. However, the intensity was small compared to the high fluorescence enhancement of the receptor in the presence of Zn^{2+}. These results indicate that receptor **1** could be used as a fluorescence chemosensor for Zn^{2+}. Importantly, **1** can clearly distinguish Zn^{2+} from Cd^{2+}, whereas the discrimination of Zn^{2+} from Cd^{2+} is well known to be a major obstacle. The selective fluorescence enhancement by Zn^{2+} might be due to the effective coordination of Zn^{2+} with **1** over other metal ions. It causes the zinc complex to be more coplanar structure than the **1** itself, resulting in the chelation-enhanced fluorescence (CHEF) effect.[22] Also, receptor **1** is poorly fluorescent in part due to isomerization of the C=N double bond in the excited state and in part due to excited-state intramolecular proton transfer (ESIPT)[23] involving the phenolic protons. Upon stable chelation with zinc

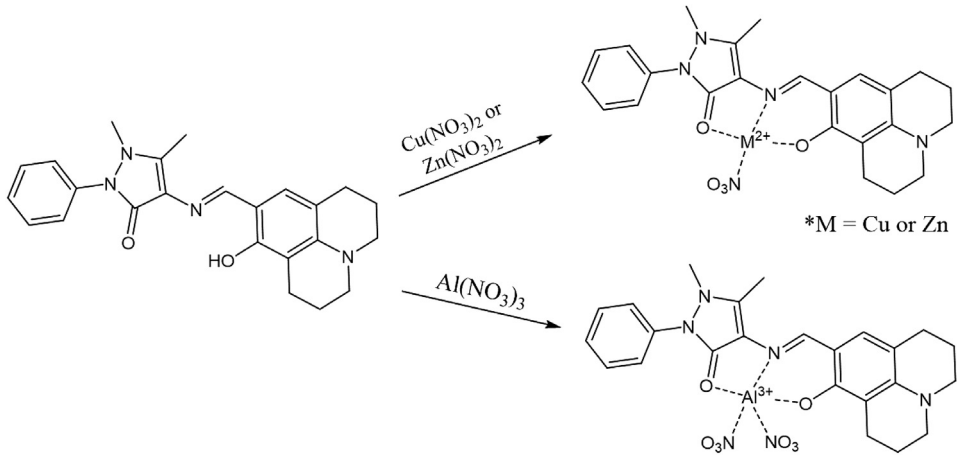

Scheme 2. The proposed structures for **1**-Cu^{2+}, **1**-Zn^{2+}, and **1**-Al^{3+} complexes.

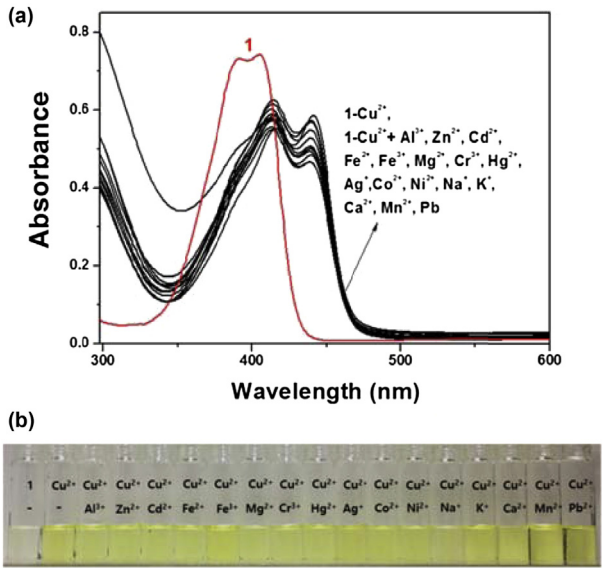

Fig. 5. (a) Competitive selectivity of **1** (20 μM) towards Cu^{2+} (4 equiv) in the presence of other metal ions (4 equiv) in DMSO-buffer solution (10 mM bis–tris, pH 7.0, 2:1, v/v). (b) Colorimetric competitive experiment of **1** (20 μM) in the presence of Cu^{2+} (4 equiv) and other metal ions (4 equiv) in DMSO-buffer solution (10 mM bis–tris, pH 7.0, 2:1, v/v).

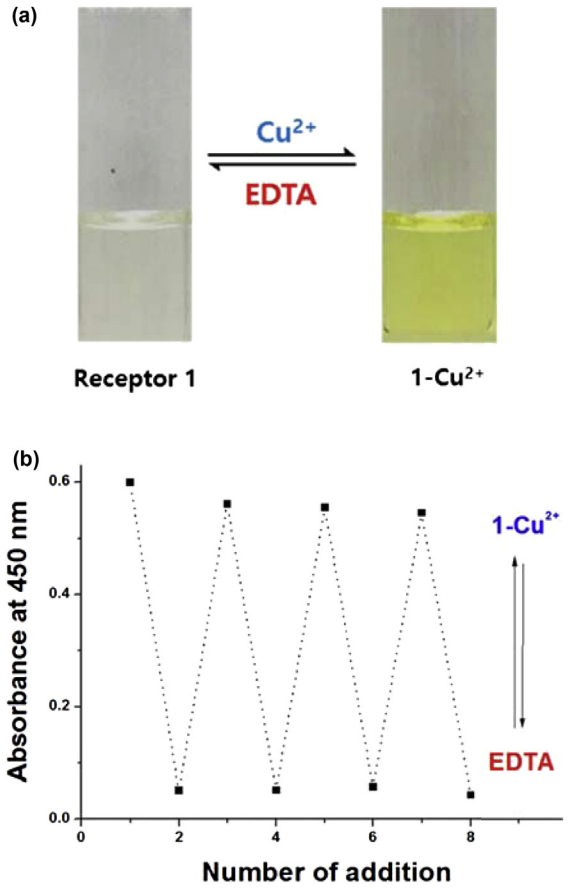

Fig. 6. (a) Colorimetric changes of **1** (20 μM) after the sequential addition of Cu^{2+} and EDTA in DMSO-buffer (2:1, v/v) solution. (b) Reversible changes in absorbance of **1** (20 μM) at 450 nm after the sequential addition of Cu^{2+} and EDTA.

ion, the C=N isomerization and ESIPT might be inhibited, leading to fluorescence enhancement.

To further investigate the chemosensing properties of **1** toward to Zn^{2+}, fluorescence titration of the receptor **1** with Zn^{2+} ion was performed (Fig. 8).

Upon the addition of Zn^{2+} to **1**, fluorescence intensity increased gradually and was saturated with 8 equiv of Zn^{2+}. The photophysical properties of **1** were also examined using UV–vis spectrometry (Fig. 9). Upon addition of Zn^{2+} ions to a solution of **1**, the absorption band at 403 nm decreased and a new absorbance intensity at 443 nm increased with an isosbestic point at 406 nm, which indicates a clean conversion of **1** into the **1**-Zn^{2+} complex.

The binding mode between **1** and Zn^{2+} was determined by using Job plot analysis. As shown in Fig. S5, the Job plot for the **1**-Zn^{2+} complex exhibited 1:1 complexation stoichiometry. The formation of **1**-Zn^{2+} complex was further confirmed by ESI-mass spectrometry analysis. The positive ion mass spectrum indicated the 1:1 binding mode between **1** and Zn^{2+} [m/z 537.73; calcd, 538.18] as shown in Fig. S6. From the results of fluorescence titration, the association constant of the **1**-Zn^{2+} complex was determined as 5.0×10^7 M^{-1} on the basis of Benesi–Hildebrand equation (Fig. S7). This value is within the range of those ($1.0–1.0\times10^{12}$) reported for Zn^{2+}-chemosensors.[11b,24] For practical application, the detection limit was also an important parameter. Thus, the detection limit ($3\sigma/k$) of receptor **1** for the analysis of Zn^{2+} ion was calculated to be 49 nM (Fig. S8).

To check the practical applicability of **1** as a selective fluorescence sensor for Zn^{2+}, the competition experiments were

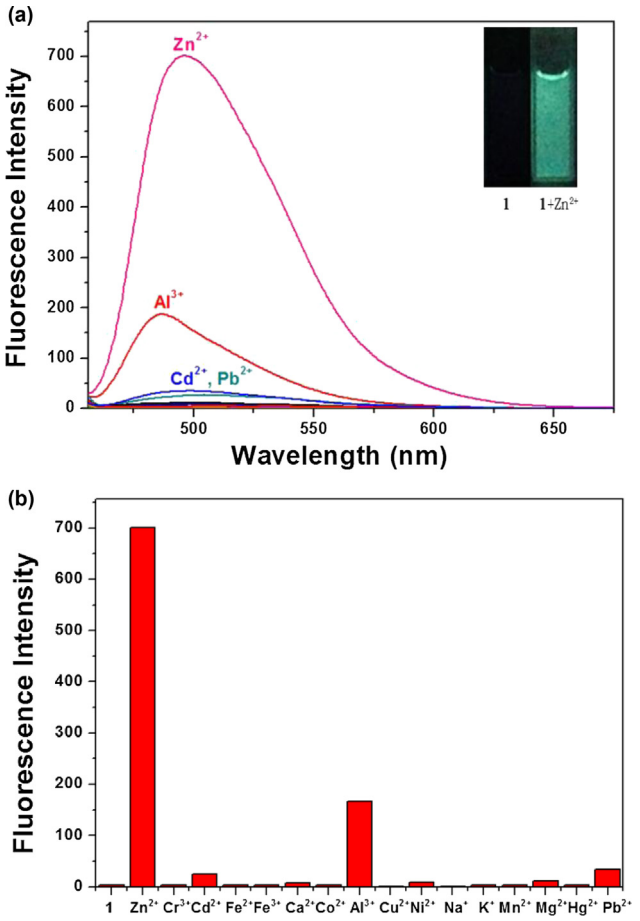

Fig. 7. (a) Fluorescence spectra changes of **1** (10 μM) in the presence of different metal ions (5 equiv) such as Na^+, K^+, Mg^{2+}, Ca^{2+}, Al^{3+}, Cr^{3+}, Mn^{2+}, Fe^{2+}, Fe^{3+}, Co^{2+}, Ni^{2+}, Zn^{2+}, Ag^+, Cd^{2+}, Hg^{2+}, and Pb^{2+} with an excitation of 430 nm in DMF. (b) Bar graph shows the relative emission intensity of **1** at 500 nm upon treatment with various metal ions.

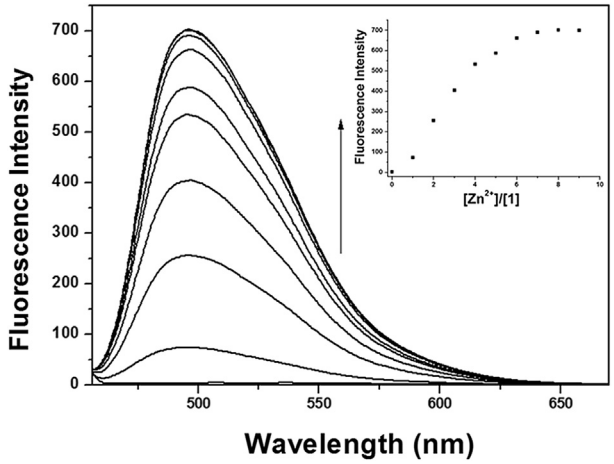

Fig. 8. Change of fluorescence spectra of receptor **1** (10 μM) upon gradual addition of Zn^{2+} in DMF. Inset: The ratio of fluorescence of **1** as a function of Zn^{2+} equiv.

conducted in the presence of Zn^{2+} mixed with other relevant metal ions, such as Na^+, K^+, Mg^{2+}, Ca^{2+}, Al^{3+}, Cr^{3+}, Mn^{2+}, Fe^{2+}, Fe^{3+}, Co^{2+}, Ni^{2+}, Ag^+, Cd^{2+}, Hg^{2+}, and Pb^{2+}. When **1** was treated with 8 equiv of Zn^{2+} in the presence of the same concentration of other metal ions (Fig. S9), the coexistent metal ions had a small and negligible effect on the emission intensity of the **1**-Zn^{2+} complexation, except

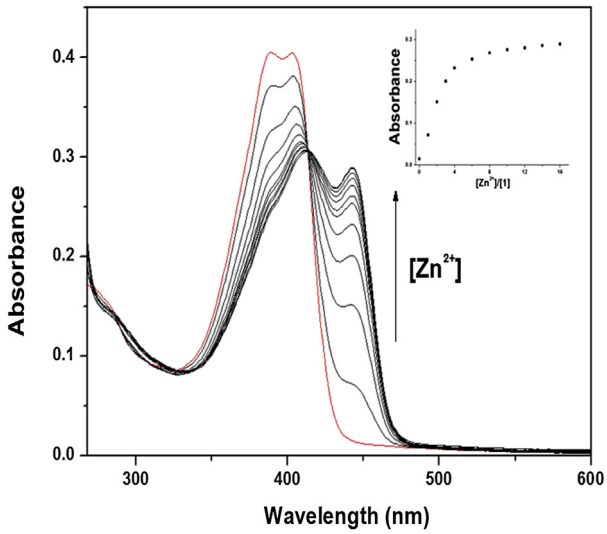

Fig. 9. UV–vis spectra of receptor **1** (10 μM) upon gradual addition of Zn^{2+} in DMF. Inset: The ratio of absorbance of **1** as a function of Zn^{2+} equiv.

for Cr^{3+}, Cu^{2+}, Fe^{2+}, Fe^{3+}, and Na^+. Cr^{3+}, Fe^{2+}, Na^+, and Fe^{3+} inhibited about 57, 71, 79 and 93% of the emission intensity, respectively, and Cu^{2+} completely interfered. Nevertheless, it is worth noting that cadmium ion hardly inhibited the fluorescence intensity of the **1**-Zn^{2+} complex. These results indicate that **1** could be a good Zn^{2+} sensor, which could distinguish Zn^{2+} from Cd^{2+} commonly having similar properties.

The interaction between receptor **1** and Zn^{2+} was further studied through ^1H NMR titration in DMF-d_7 (Fig. 10). Upon addition of 1 equiv of Zn^{2+}, the proton of the hydroxyl group at 13.2 ppm disappeared due to its deprotonation, and the H_8 of C=N moiety at 9.3 ppm was shifted to downfield by 0.1 ppm. The rest of protons were shifted to upfield. The H_6 and H_7 were shifted to upfield by 0.02 and 0.05 ppm, respectively, which suggests that the oxygen atom of the keto moiety might be involved in Zn^{2+} coordination. There was no shift in the position of proton signals on further addition of Zn^{2+} (>1 equiv). Based on the Job plot, ESI-mass spectrometry analysis, and ^1H NMR titration, we propose the structure of a 1:1 complex of **1** and Zn^{2+}, as shown in Scheme 2.

2.4. Fluorogenic sensing for Al^{3+} in MeCN

To gain an insight into the fluorescent properties of receptor **1** toward various metal ions in MeCN, the emission changes were measured with them. When excited at 390 nm, **1** exhibited a weak fluorescence emission (λ_{max}=485 nm) compared to that (1500-folds) in the presence of Al^{3+}. By contrast, upon addition of other metal ions such as Na^+, K^+, Mg^{2+}, Ca^{2+}, Ga^{3+}, In^{3+}, Cr^{3+}, Mn^{2+}, Fe^{2+}, Fe^{2+}, Co^{2+}, Ni^{2+}, Cu^{2+}, Zn^{2+}, Cd^{2+}, Hg^{2+}, and Pb^{2+} with their nitrate salts, either no or slight increase in intensity were observed (Fig. 11).

It is noteworthy that **1** could serve as an excellent fluorescent probe for Al^{3+} by switching solvents from DMF to MeCN. These results inform that the fluorescence behaviors of **1**-Zn^{2+} and **1**-Al^{3+} complexes are solvent-dependent. The dramatic fluorescence enhancement responses to Al^{3+} could be also explained by the same three mechanisms as did in **1**-Zn^{2+} complex: (1) CHEF effect; (2) the inhibition of C=N isomerization; (3) the hindrance of ESIPT process. To further investigate the chemosensing properties of **1**, a fluorimetric titration of **1** was performed with the Al^{3+} ion. As shown in Fig. 12, the emission intensity of **1** at 485 nm steadily increased until the amount of Al^{3+} reached 15 equiv. The

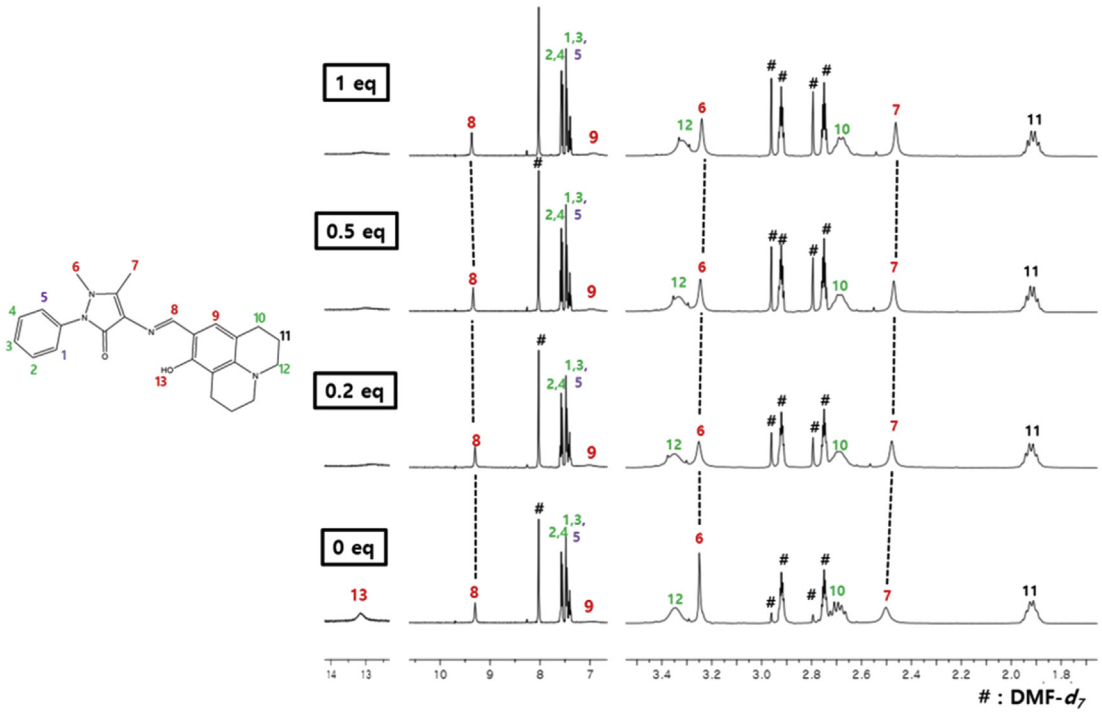

Fig. 10. ^{1}H NMR titration of receptor **1** with Zn^{2+} in DMF-d_7.

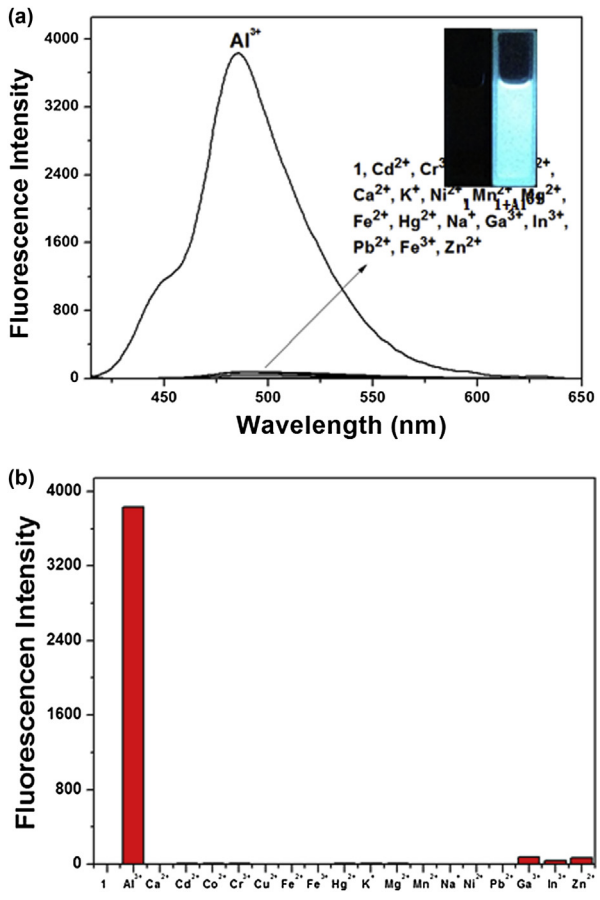

Fig. 11. (a) Fluorescence spectra changes of **1** (10 μM) in the presence of different metal ions (15 equiv) such as Na^+, K^+, Mg^{2+}, Ca^{2+}, Al^{3+},Ga^{3+}, In^{3+} Cr^{3+}, Mn^{2+}, Fe^{2+}, Fe^{3+}, Co^{2+}, Ni^{2+}, Cu^{2+}, Zn^{2+}, Cd^{2+}, Hg^{2+}, and Pb^{2+} with an excitation of 390 nm in MeCN. (b) Bar graph shows the relative emission intensity of **1** at 485 nm upon treatment with various metal ions.

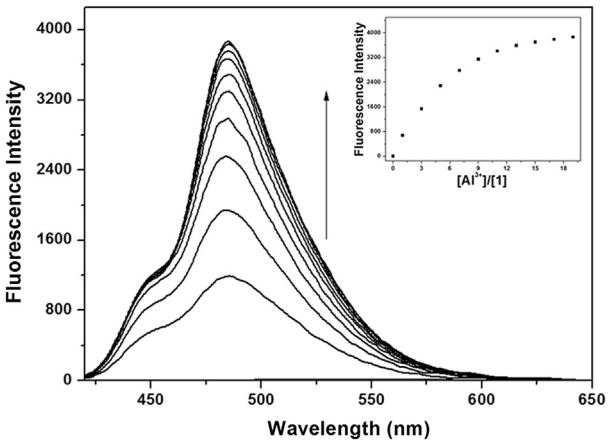

Fig. 12. Change of fluorescence spectra of receptor **1** (10 μM) upon gradual addition of Al^{3+} in MeCN. Inset: The ratio of fluorescence of **1** as a function of Al^{3+} equiv.

photophysical properties of **1** were also examined using UV–vis spectrometry. UV–vis absorption spectrum of **1** showed a broad absorbance band at the range of 388–400 nm (Fig. S10). Upon the addition of Al^{3+} ions to a solution of **1**, the broad absorbance region decreased, while a new absorption band at 441 nm increased. Meanwhile, a clear isosbestic point at 410 nm implies the undoubted conversion of free **1** to the **1**-Al^{3+} complex.

The Job plot showed a 1:1 complexation stoichiometry between **1** and Al^{3+} (Fig. S11), which was further confirmed by ESI-mass spectrometry analysis (Fig. S12). The positive-ion mass spectrum indicated that a peak at m/z=804.80 is assignable to [**1**-H^++Al^{3+}+NO_3^-+3DMF+MeCN+3H_2O]$^+$ [calcd, m/z: 804.38]. From the fluorescence titration data, the association constant for **1**-Al^{3+} complexation was determined as 1.2×10^7 M^{-1} from Benesi–Hildebrand equation (Fig. S13). This value is in the range of those (10^3–10^9) reported for Al^{3+} binding chemosensor.[25] The detection limit ($3\sigma/k$) of receptor **1** as a fluorescence sensor for the analysis of

Al^{3+} ions was found to be 14 nM (Fig. S14), which implies that **1** could sense the nanomolar level of Al^{3+}.

To further check the practical applicability of receptor **1** as Al^{3+} selective fluorescent sensor, we carried out competition experiments. Compound **1** was treated with 15 equiv of Al^{3+} in the presence of other metal ions of the same concentration (Fig. S15). Unfortunately, Al^{3+} complexation with receptor **1** was inhibited completely by Cu^{2+} and Fe^{2+}, which are well known as the strong quenchers of fluorescence, and Cr^{3+}, Fe^{3+}, Hg^{2+}, In^{3+}, K^{+}, Mg^{2+}, Na^{+}, and Pb^{2+} did more than 50% of it.

In order to further investigate binding mode between **1** and Al^{3+}, ^1H NMR titration was conducted in DMF-d_7 (Fig. 13). Upon addition of 1 equiv of Al^{3+}, the proton of phenol moiety (H_{13}) became disappeared completely. The protons of methyl groups (H_6 and H_7) were shifted to upfield by 0.02 and 0.04, respectively. The imine proton (H_8) was shifted to downfield by 0.04, while other protons in **1** changed little. These results indicate that Al^{3+} might be coordinated to two oxygen atoms of keto and phenol groups and nitrogen of imine moiety, as proposed in Scheme 2. On further addition of Al^{3+} (>1 equiv) into **1** solution, no shift in the position of proton signals was observed, which supports a 1:1 complexation of **1** with Al^{3+}.

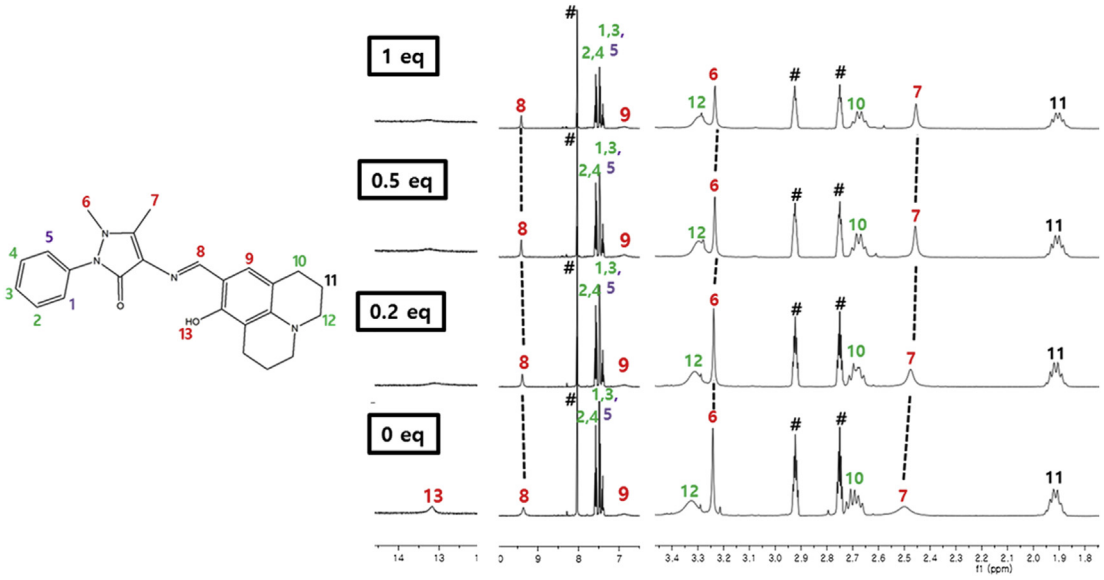

Fig. 13. ^1H NMR titration of receptor **1** with Al^{3+} in DMF-d_7.

3. Conclusion

We have developed a new chemosensor **1** based on Schiff base with julolidine and antipyrine moieties. The formulation and detailed structural characterizations of **1** have been established by using spectroscopic and single crystal X-ray crystallographic tools. Compound **1** can be used as a multifunctional chemosensor for highly selective detection of Cu^{2+}, Al^{3+} and Zn^{2+} depending on solvents. It distinguished Cu^{2+} ion from other metal ions by color change in aqueous media without expensive equipment. The binding of the receptor **1** and Cu^{2+} was also chemically reversible with EDTA. Moreover, receptor **1** could be used as a fluorogenic chemosensor for Zn^{2+} and Al^{3+} ions in DMF and MeCN solutions, respectively. Furthermore, the receptor **1** has the very low detection limits (49 and 14 nM) of Zn^{2+} and Al^{3+}, respectively, in different organic solvents, which implies that **1** could sense the nanomolar level of these metal ions. Consequently, **1** showed the possibility to be used as a dual-mode sensor for three different metal ions in different solvents.

4. Experimental

4.1. Materials and instrumentation

All the solvents and reagents (analytical grade and spectroscopic grade) were obtained from Sigma–Aldrich and used as received. NMR spectra were recorded on a Varian 400 spectrometer. Chemical shifts (δ) are reported in parts per million, relative to tetramethylsilane $Si(CH_3)_4$. Absorption spectra were recorded at room temperature using a Perkin Elmer model Lambda 2S UV/Vis spectrometer. Electrospray ionization mass spectra (ESI-mass) were collected on a Thermo Finnigan (San Jose, CA, USA) LCQTM Advantage MAX quadrupole ion trap instrument. Fluorescence measurements were performed on a Perkin Elmer model LS45 fluorescence spectrometer. Elemental analysis for carbon, nitrogen, and hydrogen was carried out by using a Flash EA 1112 elemental analyzer (thermo) in Organic Chemistry Research Center of Sogang University, Korea.

4.2. Synthesis of 1

The receptor **1** was prepared by the condensation reaction of 8-hydroxyjulolidine-9-carboxaldehyde with 4-aminoantipyrine (Scheme 1). To an ethanol (10 mL) solution of 8-hydroxyjulolidine-9-carboxaldehyde (0.26 g, 1.2 mmol), two drops of HCl and 4-aminoantipyrine (0.20 g, 1 mmol) in ethanol (5 mL) were added slowly while being stirred vigorously. After 5 h, the yellow product was recrystallized from diethyl ether. The resulting precipitate was filtered and washed five times with ice ethanol (0.33 g, 82%). The solid compound **1** (0.04 g, 0.1 mmol) dissolved in methanol (8 mL) was evaporated slowly to get yellow crystals suitable for X-ray analysis for a week. Mp: 242–244 °C. ^1H NMR (400 MHz, $CDCl_3$) δ 11.92 (s, 1H), 9.00 (s, 1H), 7.52 (t, J=8 Hz, 2H), 7.39 (m, 3H), 6.76 (s, 1H), 3.38 (m, 4H), 3.19 (s, 3H), 3.09 (t, J=6 Hz, 2H), 2.65 (t, J=6 Hz, 2H), 2.47 (s, 3H), 1.97 (m, 4H). ESI-MS m/z $[M+H]^+$: calcd, 403.20; found, 403.31. Anal. Calcd for

$C_{24}H_{26}N_4O_2$: C, 71.62; H, 6.51; N, 13.92%. Found: C, 71.28; H, 6.64; N, 13.51%.

4.3. X-ray data collection and structure determination

A yellow block-type crystal, approximate dimensions 0.20 mm×0.20 mm×0.12 mm, was used for the X-ray crystallographic analysis. The diffraction data for the compound was collected on a Bruker SMART APEX diffractometer equipped with a monochromator in the Mo Ka (k=0.71073 Å) incident beam. The crystal was mounted on a silicone loop and collected data at 170 K. The CCD data were integrated and scaled using the Bruker-SAINT software package, and the structure was solved and refined using SHEXTL V6.12. All hydrogen atoms except imine hydrogen atom were located in the calculated positions. The crystallographic data are listed in Table 1. The bond lengths and angles are listed in Table S1. Structural information was deposited at the Cambridge Crystallographic Data Center (CCDC 1001739).

Table 1
Crystal data and structure refinement for **1**

Empirical formula	$C_{24}H_{27}ClN_4O_2$	
Formula weight	438.95	
Temperature	170(2) K	
Wavelength	0.71073 Å	
Crystal system	Triclinic	
Space group	P-1	
Unit cell dimensions	a=8.3140(17) Å	α=89.66(3)°
	b=9.3540(19) Å	β=76.82(3)°
	c=15.720(3) Å	γ=66.15(3)°
Volume	1083.6(4) Å^3	
Z	2	
Density (calculated)	1.345 Mg/m^3	
Absorption coefficient	0.206 mm^{-1}	
F(000)	464	
Crystal size	0.20×0.20×0.12 mm^3	
Theta range for data collection	1.34–26.00°	
Index ranges	$-10\le h\le 10$, $-11\le k\le 11$, $-10\le l\le 19$	
Reflections collected	6173	
Independent reflections	4161 [R(int)=0.0366]	
Completeness to theta=26.00?	97.7%	
Absorption correction	Multi-scan	
Max. and min. transmission	0.9757 and 0.9600	
Refinement method	Full-matrix least-squares on F^2	
Data/restraints/parameters	4161/0/286	
Goodness-of-fit on F^2	1.099	
Final R indices [$I>2\sigma(I)$]	R_1=0.0516, wR_2=0.1376	
R indices (all data)	R_1=0.0689, wR_2=0.1447	
Largest diff. peak and hole	0.575 and −0.427 e Å^{-3}	

4.4. Chromogenic Cu(II) sensing

4.4.1. UV–vis titration in DMSO-buffer solution. The receptor **1** (4.0 mg, 0.01 mmol) was dissolved in DMSO (1 mL) and 6 μL of the **1** (10 mM) were diluted to 2.994 mL of DMSO-buffer solution (2:1, v/v, 10 mM bis-tris, pH 7.0) to make the concentration of 20 μM. $Cu(NO_3)_2$ (0.005 mmol) was dissolved in DMSO (1 mL). 3–48 μL of the Cu^{2+} solution (5 mM) were transferred to the receptor solution (20 μM, 3 mL) prepared above. After mixing them for a few seconds, UV–vis spectra were taken at room temperature.

4.4.2. Job plot measurement with UV–vis in DMSO-buffer solution. The receptor **1** (4.0 mg, 0.01 mmol) and $Cu(NO_3)_2$ (0.01 mmol) were dissolved in DMSO (1 mL), respectively. 6 μL of the receptor **1** solution were diluted to 39.4 mL of DMSO-buffer solution (2:1, v/v, 10 mM bis-tris, pH 7.0) to make the concentration of 20 μM. The $Cu(NO_3)_2$ solution was diluted in the same way. 5.0, 4.5, 4.0, 3.5, 3.0, 2.5, 2.0, 1.5, 1.0, 0.5 and 0 mL of the receptor **1** solution were taken and transferred to vials. 0, 0.5, 1.0, 1.5, 2.0, 2.5, 3.0, 3.5, 4.0, 4.5 and 5.0 mL of the Cu^{2+} solution were added to each receptor solution separately. Each vial had a total volume of 5 mL. After shaking the vials for a few seconds, UV–vis spectra were taken at room temperature.

4.4.3. Competitive experiments. The receptor **1** (4.0 mg, 0.01 mmol) was dissolved in DMSO (1 mL). MNO_3 (M=Na, K, Ag, 0.01 mmol) or $M(NO_3)_2$ (M=Mn, Co, Ni, Cu, Zn, Cd, Mg, Ca, Hg, Pb, 0.01 mmol) or $M(NO_3)_3$ (M=Al, Fe, Cr, 0.01 mmol) or $M(ClO_4)_2$ (M=Fe, 0.01 mmol) were dissolved in DMSO (1 mL), respectively. 24 μL of each metal solution (10 mM) were diluted to 2.946 mL of DMSO-buffer solution (2:1, v/v, 10 mM bis–tris, pH 7.0), separately. 24 μL of the Cu^{2+} solution (10 mM) were taken and added to the solutions prepared above. Then, 6 μL (1 mM) of the **1** were taken and added to the mixed solutions. Each vial had a total volume of 3 mL. After shaking the vials for a few seconds, UV–vis spectra were taken at room temperature.

4.5. Fluoregenic Zn(II) sensing

4.5.1. Fluorescence titration in DMF. The receptor **1** (4.0 mg, 0.01 mmol) was dissolved in DMF (1 mL) and 3 μL of the **1** (10 mM) were diluted to 2.997 mL of DMF to make the concentration of 10 μM. $Zn(NO_3)_2$ was also dissolved in DMF (1 mL) and 3–27 μL of the Zn^{2+} solution (10 mM) were transferred to the solution of **1** (10 μM, 3 mL) prepared above. After mixing them for a few seconds, fluorescence spectra were taken at room temperature.

4.5.2. UV–vis titration in DMF. The receptor **1** (4.0 mg, 0.01 mmol) was dissolved in DMF (1 mL) and 3 μL of the **1** (10 mM) were diluted to 2.997 mL of DMF to make the concentration of 10 μM. $Zn(NO_3)_2$ (0.01 mmol) was also dissolved in DMF (1 mL) and 3–51 μL of the Zn^{2+} solution (5 mM) were transferred to the solution of **1** (10 μM, 3 mL) prepared above. After mixing them for a few seconds, UV–vis spectra were taken at room temperature.

4.5.3. Job plot measurement in DMF. The receptor **1** (4.0 mg, 0.01 mmol) was dissolved in DMF (1 mL) and 3 μL of the receptor **1** solution were diluted to 2.997 mL of DMF to make the concentration of 10 μM. $Zn(NO_3)_2$ solution was also dissolved and diluted in the same way. 5.0, 4.5, 4.0, 3.5, 3.0, 2.5, 2.0, 1.5, 1.0, 0.5 and 0 mL of the receptor **1** solution were taken and transferred to vials. 0, 0.5, 1.0, 1.5, 2.0, 2.5, 3.0, 3.5, 4.0, 4.5 and 5.0 mL of the Zn^{2+} solution were transferred to each receptor solution, respectively. Each vial had a total volume of 5 mL. After shaking the vials for a few seconds, fluorescence spectra were taken at room temperature.

4.5.4. Competitive experiments in DMF. The receptor **1** (4.0 mg, 0.01 mmol) was dissolved in DMF (1 mL). MNO_3 (M=Na, K, 0.1 mmol) or $M(NO_3)_2$ (M=Mn, Co, Ni, Cu, Zn, Cd, Mg, Ca, Hg, Pb, 0.1 mmol) or $M(NO_3)_3$ (M=Al, Fe, Cr, 0.1 mmol) or $M(ClO_4)_2$ (M=Fe, 0.1 mmol) were dissolved in DMF (1 mL), respectively. 24 μL of each metal solution (10 mM) were diluted to 2.949 mL of DMF, separately. 24 μL of the Zn^{2+} solution (10 mM) were taken and added to the solutions prepared above. Then, 3 μL of the **1** (10 mM) were taken and added to the mixed solutions. Each vial had a total volume of 3 mL. After shaking the vials for a few seconds, fluorescence spectra were taken at room temperature.

4.5.5. NMR titration with Zn^{2+} ion. Four NMR tubes of **1** (0.80 mg, 0.002 mmol) dissolved in DMF-d_7 (0.7 mL) were prepared, and four different equiv (0, 0.25, 0.5 and 1 equiv) of the $Zn(NO_3)_2$ dissolved

in DMF-d_7 (0.3 mL) were added to the **1** solution, respectively. After shaking them for a minute, their ^{1}H NMR spectra were taken.

4.6. Fluoregenic Al(III) sensing

4.6.1. Fluorescence titration in MeCN. The receptor **1** (4.0 mg, 0.01 mmol) was dissolved in DMF (1 mL) and 3 μL (10 mM) of **1** were diluted to 2.997 mL of MeCN to make the concentration of 10 μM. $Al(NO_3)_3$ was also dissolved in DMF (1 mL) and 4.5–57 μL of the Al^{3+} solution (10 mM) were transferred to the solution of **1** (10 μM, 3 mL) prepared above. After mixing them for a few seconds, fluorescence spectra were taken at room temperature.

4.6.2. UV–vis titration in MeCN. The receptor **1** (4.0 mg, 0.01 mmol) was dissolved in DMF (1 mL) and 3 μL (10 mM) of **1** were diluted to 2.997 mL of MeCN to make the concentration of 10 μM. $Al(NO_3)_3$ (0.01 mmol) was also dissolved in DMF (1 mL) and 4.5–57 μL of the Al^{3+} solution (10 mM) were transferred to the solution of **1** (10 μM, 3 mL) prepared above. After mixing them for a few seconds, UV–vis spectra were taken at room temperature.

4.6.3. Job plot measurement in MeCN. The receptor **1** (4.0 mg, 0.01 mmol) was dissolved in DMF (1 mL). 3 μL of the receptor **1** solution were diluted to 2.997 mL of MeCN to make the concentration of 10 μM. $Al(NO_3)_3$ solution was also dissolved and diluted in the same way. 5.0, 4.5, 4.0, 3.5, 3.0, 2.5, 2.0, 1.5, 1.0, 0.5 and 0 mL of the receptor **1** solution were taken and transferred to vials. 0, 0.5, 1.0, 1.5, 2.0, 2.5, 3.0, 3.5, 4.0, 4.5 and 5.0 mL of the Al^{3+} solution were transferred to each receptor solution, respectively. Each vial had a total volume of 5 mL. After shaking the vials for a few seconds, fluorescence spectra were taken at room temperature.

4.6.4. Competitive experiments in MeCN. The receptor **1** (4.0 mg, 0.01 mmol) was dissolved in DMF (1 mL). MNO_3 (M=Na, K, 0.1 mmol) or $M(NO_3)_2$ (M=Mn, Co, Ni, Cu, Zn, Cd, Mg, Ca, Hg, Pb, 0.1 mmol) or $M(NO_3)_3$ (M=Al, Ga, In, Fe, Cr, 0.1 mmol) or $M(ClO_4)_2$ (M=Fe, 0.1 mmol) were dissolved in DMF (5 mL), respectively. 45 μL of each metal solution (10 mM) were diluted to 2.907 mL of MeCN, separately. 45 μL of the Al^{3+} solution (10 mM) were taken and added to the solutions prepared above. Then, 3 μL (10 mM) of the **1** were taken and added to the mixed solutions. Each vial had a total volume of 3 mL. After shaking the vials for a few seconds, fluorescence spectra were taken at room temperature.

4.6.5. NMR titration with Al^{3+} ion. Four NMR tubes of **1** (0.80 mg, 0.002 mmol) dissolved in DMF-d_7 (0.7 mL) were prepared, and four different equiv (0, 0.25, 0.5 and 1 equiv) of the $Al(NO_3)_3$ dissolved in DMF-d_7 (0.3 mL) were added to the **1** solution, respectively. After shaking them for a minute, their ^{1}H NMR spectra were taken.

Acknowledgements

Financial support from Basic Science Research Program through the National Research Foundation of Korea (NRF) funded by the Ministry of Education, Science and Technology (2012001725 and 2012008875) are gratefully acknowledged.

Supplementary data

Additional experimental data are available. Supplementary data related to this article can be found at http://dx.doi.org/10.1016/j.tet.2014.08.026.

References and notes

1. Rao, K. S.; Balaji, T.; Rao, T. P.; Babu, Y.; Naidu, G. R. K. *Spectrochim. Acta, Part B* **2002**, *57*, 1333–1338.
2. Sturgeon, R. E.; Berman, S. S. *Anal. Chem.* **1979**, *51*, 2364–2369.
3. Gulaboski, R.; Mirčeski, V.; Scholz, F. *Electrochem. Commun.* **2002**, *4*, 277–283.
4. (a) Chen, Y.; Mi, Y.; Xie, Q.; Xiang, J.; Fan, H.; Luo, X.; Xia, S. *Anal. Methods* **2013**, *5*, 4818–4823; (b) Jiayu, J.; Junji, Z.; Lei, Z.; He, T. *Analyst* **2013**, *138*, 1641–1644; (c) Qi, Z.; Xin, L.; Junji, Z.; Ji, Z.; Bingbing, S.; He, T. *Chem. Commun.* **2012**, 2095–2097.
5. (a) Kim, J. H.; Hwang, I. H.; Jang, S. P.; Kang, J.; Kim, S.; Noh, I.; Kim, Y.; Kim, C.; Harrison, R. G. *Dalton Trans.* **2013**, *42*, 5500–5507; (b) Song, E. J.; Kang, J.; You, G. R.; Park, G. J.; Kim, Y.; Kim, S.; Kim, C.; Harrison, R. G. *Dalton Trans.* **2013**, *42*, 15514–15520; (c) Valeur, B.; Leray, I. *Coord. Chem. Rev.* **2000**, *205*, 3–40; (d) Kim, K. B.; Kim, H.; Song, E. J.; Kim, S.; Noh, I.; Kim, C. *Dalton Trans.* **2014**, *43*, 3999–4008; (f) Domaille, D. W.; Que, E. L.; Chang, C. J. *Nat. Chem. Biol.* **2008**, *4*, 168–175.
6. (a) Wang, J.; Lin, W.; Li, W. *Chem.—Eur. J.* **2012**, *18*, 13629–13632; (b) Liu, X.; Zhang, N.; Zhou, J.; Chang, T.; Fanga, C.; Shangguan, D. *Analyst* **2013**, *138*, 901–906; (c) Yeo, H. M.; Ryu, B. J.; Nam, K. C. *Org. Lett.* **2008**, *10*, 2931–2934.
7. (a) Chen, X.; Jou, M. J.; Lee, H.; Kou, S.; Lim, J.; Nam, S.; Park, S.; Kim, K.; Yoon, J. *Sens. Actuators, B* **2009**, *137*, 597–602; (b) Uauy, R.; Olivares, M.; Gonzalez, M. *Am. J. Clin. Nutr.* **1998**, *67*, 952S–959S.
8. (a) Yin, S.; Leen, V.; Snick, S. V.; Boens, N.; Dehaen, W. *Chem. Commun.* **2010**, 6329–6331; (b) Yu, F.; Zhang, W.; Li, P.; Xing, Y.; Tong, L.; Ma, J.; Tang, B. *Analyst* **2009**, *134*, 1826–1833; (c) Liu, J.; Lu, Y. *Chem. Commun.* **2007**, 4872–4874; (d) Jung, H. S.; Kwon, P. S.; Lee, J. W.; Kim, J. I.; Hong, C. S.; Kim, J. W.; Yan, S.; Lee, J. Y.; Lee, J. H.; Joo, T.; Kim, J. S. *J. Am. Chem. Soc.* **2009**, *131*, 2008–2012.
9. (a) Lim, N. C.; Yao, L.; Freake, H. C.; Bruckner, C. *Bioorg. Med. Chem. Lett.* **2003**, *13*, 2251–2254; (b) Jiang, P.; Guo, Z. *Coord. Chem. Rev.* **2004**, *248*, 205–229; (c) Choi, J. Y.; Kim, D.; Yoon, J. *Dyes Pigm.* **2013**, *96*, 176–179; (d) Wang, F.; Moon, J. H.; Nandhakumar, R.; Kang, B.; Kim, D.; Kim, K. M.; Lee, J. Y.; Yoon, J. *Chem. Commun.* **2013**, 7228–7230.
10. (a) Park, M. S.; Swamy, K. M. K.; Lee, Y. J.; Lee, H. N.; Jang, Y. J.; Moon, Y. H.; Yoon, J. *Tetrahedron Lett.* **2006**, *47*, 8129–8132; (b) Xu, Z.; Kim, G.; Han, S. J.; Jou, M. J.; Lee, C.; Shin, I.; Yoon, J. *Tetrahedron* **2009**, *65*, 2307–2312; (c) Åstrand, O. A. H.; Austdal, L. P. E.; Paulsen, R. E.; Hansen, T. V.; Rongved, P. *Tetrahedron* **2013**, *69*, 8645–8654; (d) Lee, H. G.; Kim, K. B.; Park, G. J.; Na, Y. J.; Jo, H. Y.; Lee, S. A.; Kim, C. *Inorg. Chem. Commun.* **2014**, *39*, 61–65; (e) Lee, H. G.; Lee, J. H.; Jang, S. P.; Hwang, I. H.; Kim, S.; Kim, Y.; Kim, C.; Harrison, R. G. *Inorg. Chim. Acta* **2013**, *394*, 542–551; (f) Li, K.; Tong, A. *Sens. Actuators, B* **2013**, *184*, 248–253; (g) Shellaiah, M.; Wu, Y.; Lin, H. *Analyst* **2013**, *138*, 2931–2942.
11. (a) Li, Y.; Zhao, Q.; Yang, H.; Liu, S.; Liu, X.; Zhang, Y.; Hu, T.; Chen, J.; Chang, Z.; Bu, X. *Analyst* **2013**, *138*, 5486–5494; (b) Xu, Z.; Yoon, J.; Spring, D. R. *Chem. Soc. Rev.* **2010**, *39*, 1996–2006; (c) Yan, M.; Li, T.; Yang, Z. *Inorg. Chem. Commun.* **2011**, *14*, 463–465; (d) Kim, H.; Kang, J.; Kim, K. B.; Song, E. J.; Kim, C. *Spectrochim. Acta, Part A* **2014**, *118*, 883–887.
12. (a) Nayak, P. *Environ. Res.* **2002**, *89*, 101–115; (b) Fasman, G. D. *Coord. Chem. Rev.* **1996**, *149*, 125–165; (c) Exley, C. *Coord. Chem. Rev.* **2012**, *256*, 2142–2146; (d) Berthon, G. *Coord. Chem. Rev.* **2002**, *228*, 319–341.
13. (a) Kadarkaraisamy, M.; Madhubabu, A.; Gerald, C.; Vinothini, B.; Mariah, M. H.; Mikaela, H.; Andrew, G. S. *Inorg. Chem.* **2014**, *53*, 2953–2962; (b) Ma, Y.; Chen, H.; Wang, F.; Kambam, S.; Wang, Y.; Mao, C.; Chen, X. *Dyes Pigm.* **2014**, *102*, 301–307; (c) Kim, S.; Noh, J. Y.; Kim, K. Y.; Kim, J. H.; Kang, H. K.; Nam, S.; Kim, S. H.; Park, S.; Kim, C.; Kim, J. *Inorg. Chem.* **2012**, *51*, 3597–3602.
14. (a) Wang, L.; Li, H.; Cao, D. *Sens. Actuators, B* **2013**, *181*, 749–755; (b) Wang, M.; Wang, J.; Xue, W.; Wu, A. *Dyes Pigm.* **2013**, *97*, 475–480; (c) Basa, P. N.; Sykes, A. G. *J. Org. Chem.* **2012**, *77*, 8428–8434; (d) Jung, H. J.; Singh, N.; Lee, D. Y.; Jang, D. O. *Tetrahedron Lett.* **2010**, *51*, 3962–3965; (e) Liu, A.; Yang, L.; Zhang, Z.; Zhang, Z.; Xu, D. *Dyes Pigm.* **2013**, *99*, 472–479.
15. (a) Jung, J. Y.; Han, S. J.; Chun, J.; Lee, C.; Yoon, J. *Dyes Pigm.* **2012**, *94*, 423–426; (b) Tang, L.; Li, F.; Liu, M.; Nandhakumar, R. *Spectrochim. Acta, Part A* **2011**, *78*, 1168–1172; (c) Swamy, K. M. K.; Kim, M. J.; Jeon, H. R.; Jung, J. Y.; Yoon, J. *Bull. Korean Chem. Soc.* **2010**, *31*, 3611–3616.
16. (a) Maity, D.; Manna, A. K.; Karthigeyan, D.; Kundu, T. K.; Pati, S. K.; Govindaraju, T. *Chem.—Eur. J.* **2011**, *17*, 11152–11161; (b) Noh, J. Y.; Kim, S.; Hwang, I. H.; Lee, G. Y.; Kang, J.; Kim, S. H.; Min, J.; Park, S.; Kim, C.; Kim, J. *Dyes Pigm.* **2013**, *99*, 1016–1021; (c) Lee, S. A.; You, G. R.; Choi, Y. W.; Jo, H. Y.; Kim, A. R.; Noh, I.; Kim, S.; Kim, Y.; Kim, C. *Dalton Trans.* **2014**, *43*, 6650–6659; (d) Park, G. J.; Hwang, I. H.; Song, E. J.; Kim, H.; Kim, C. *Tetrahedron* **2014**, *70*, 2822–2828; (e) Kim, K. B.; You, D. M.; Jeon, J. H.; Yeon, Y. H.; Kim, J. H.; Kim, C. *Tetrahedron Lett.* **2014**, *55*, 1347–1352; (f) Park, G. J.; Na, Y. J.; Jo, H. Y.; Lee, S. A.; Kim, C. *Dalton Trans.* **2014**, *43*, 6618–6622; (g) Park, G. J.; Lee, M. M.; You, G. R.; Choi, Y. W.; Kim, C. *Tetrahedron Lett.* **2014**, *55*, 2517–2522.
17. (a) Wu, J.; Wang, P.; Zhang, X.; Wu, S. *Spectrochim. Acta, Part A* **2006**, 749–752; (b) Jiang, X.; Wang, B.; Yang, Z.; Liu, Y.; Li, T.; Liu, Z. *Inorg. Chem. Commun.* **2011**, *14*, 1224–1227; (C) You, Q.; Chan, P.; Chan, W.; Hau, S. C. K.; Lee, A. W. M.; Mak, N. K.; Mak, T. C. W.; Wong, R. N. S. *RSC Adv.* **2012**, *2*, 11078–11083; (d) Dessingou, J.; Tabbasum, K.; Mitra, A.; Hinge, V. K.; Rao, C. P. *J. Org. Chem.* **2012**, *77*, 1406–1413; (e) Wu, J.; Zhou, J.; Wang, P.; Zhang, X.; Wu, S. *Org. Lett.* **2005**, *7*, 2133–2136.
18. Kaur, P.; Sareen, D.; Singh, K. *Talanta* **2011**, *83*, 1695–1700.
19. Hassan, H.; Hannaneh, F.; Rahman, B.; Peter, M. *Inorg. Chim. Acta* **2013**, *394*, 526–534.
20. (a) Xiang, Y.; Tong, A.; Jin, P.; Ju, Y. *Org. Lett.* **2006**, *8*, 2863–2866; (b) Wu, S.; Du, K.; Sung, Y. *Dalton Trans.* **2010**, *39*, 4363–4368; (c) Wu, G. H.; Wang, D. X.; Wu, D. Y.; Gao, Y.; Wang, Z. Q. *J. Chem. Sci.* **2009**, *121*, 543–548.

21. WHO. *WHO Guidelines Values for Chemicals that Are of Health Significance in Drinking Water*, 3rd ed.; Guidelines for Drinking Water Quality: Geneva, 2008.
22. Lim, N. C.; Shuster, J. V.; Porto, M. C.; Tanudra, M. A.; Yao, L.; Freake, H. C.; Brückner, C. *Inorg. Chem.* **2005**, *45*, 2018–2030.
23. Wang, L.; Qin, W.; Tang, X.; Dou, W.; Liu, W. *J. Phys. Chem. A* **2011**, *115*, 1609–1616.
24. Das, S.; Dutta, M.; Das, D. *Anal. Methods* **2013**, *5*, 6262–6285.
25. (a) Park, H. M.; Oh, B. N.; Kim, J. H.; Qiong, W.; Hwang, I. H.; Jung, K.; Kim, C.; Kim, J. *Tetrahedron Lett.* **2011**, *52*, 5581–5584; (b) Maity, D.; Govindaraju, T. *Chem. Commun.* **2010**, 4499–4501; (c) Wang, Y.; Yu, M.; Yu, Y.; Bai, Z.; Shen, Z.; Li, F. *Tetrahedron Lett.* **2009**, *50*, 6169–6172; (d) Kim, S. H.; Choi, H. S.; Kim, J.; Lee, S. J.; Quang, D. T.; Kim, J. S. *Org. Lett.* **2010**, *12*, 560–563.